Morphology Evolution of Double Fold Hexagonal Dendrites of Copper(I) Sulfide with D6h Symmetry

ARTICLE *in* CRYSTAL GROWTH & DESIGN · DECEMBER 2009

Impact Factor: 4.89 · DOI: 10.1021/cg9006263

6 AUTHORS, INCLUDING:

Zhen Fang
Anhui Normal University
57 PUBLICATIONS **989** CITATIONS

SEE PROFILE

DOI: 10.1021/cg9006263

CRYSTAL GROWTH & DESIGN
Communication
2010, Vol. 10
469–474

Morphology Evolution of Double Fold Hexagonal Dendrites of Copper(I) Sulfide with D_{6h} Symmetry

Zhen Fang,*[,†] Xueying Wang,[†] Jianmin Shen,*[,‡] Xiu Lin,[†] Yonghong Ni,[†] and Xianwen Wei[†]

[†]*Anhui Key Laboratory of Functional Molecular Solids, College of Chemistry and Materials Science, Anhui Normal University, Wuhu, 241000, P. R. China and* [‡]*School of Chemical and Biomedical Engineering, Nanyang Technological University, 637459, Singapore*

Received June 7, 2009; Revised Manuscript Received December 21, 2009

ABSTRACT: Double fold hexagonal dendrites (DFHD) of copper(I) sulfide with D_{6h} point group symmetry were synthesized by an ammonia-assisted hydrothermal process. The growth direction of the branches in DFHD could be tuned by adjusting the concentration of reagents, such as Cu^{2+} and NH_3. Studies show that the coordination effect between copper anion and ammonia ligands plays a crucial role in the formation of the final dendritic structure. The influences of the reaction temperature and time on the morphology of the product have been also discussed. A possible formation process of this novel DFHD has been proposed on the basis of experiments.

Introduction. Dendrites, with highly symmetric and ingenious branched structures, have received intensive research interests in mathematics, physics, and chemistry for centuries.[1−3] Nowadays, it is widely accepted that dendrites are created by the instability of the growing surface when the system is far from equilibrium.[4−7] Therefore, controlling the surface kinetics, such as the transport of mass and heat, which plays a key role in determining crystal structures, may result in complicated crystal growth patterns. Many reports have described the dendrite growth under supersaturating-based crystallization.[8−12] However, controlling the dendrite growth and fabricating various dendritic morphologies under medium conditions, which may have potential applications in optics, electronics, and mechanics fields,[13−16] still remains a challenge.

Copper sulfide is an important *p*-type semiconductor with a bandgap of 1.2−2.0 eV, which exhibits fast-ion conduction at high temperature.[17] Moreover, it was also found that a copper sulfide layer could be used to substitute for the CuO layer in superconductors to construct a new type of layered oxysulfide.[18] Generally, copper sulfide can easily form a series of nonstoichiometric compounds, Cu_xS (x = 1−2), with a crystal structure varying from orthogonal to hexagonal. The abundant component and crystal phase of copper sulfide result in unique properties that potentially enable it to be applicable in thermoelectric cooling material, optical filer, optical recording material, solar cell superionic material, nanoswitches, photoelectric transformers, sensors, etc.[19,20] So far, many methods have been developed to prepare Cu_xS nanomaterials, such as hydrothermal, γ-radiation, microemulsion, sonochemical, solventless, template-assisted, and thermolysis techniques.[21−30] The solubility of copper sulfides in aqueous solution are so small (Cu_2S, pK_{sp} = 47.60; CuS, pK_{sp} = 35.20)[31] that nucleation and precipitation take place even at higher temperature, which often result in products with undesirable morphologies and structures. For this reason, it is difficult to prepare copper sulfide with uniform structures. Recently, Yu et al. reported the synthesis of complex concaved cuboctahedrons of copper sulfide crystals through a solution reaction in ethylene glycol.[32] The result demonstrates that the complex crystalline structures with high geometrical symmetry could be obtained via a simple solvothermal reaction.

In previous reports, uniform copper sulfide nanostructures were usually obtained via the assistance of organic chelating agents, including ethylenediamine, ethylene glycol, or hexadecylamine.[17,24,32] The formation of coordination ions in solution can control the morphology of the final products by adjusting the nucleation rate. In this paper, instead of organic ligand, we use ammonia as stabilizer to synthesize copper(I) sulfide with an unconventional double fold hexagonal dendritical (DFHD) structure.

Experimental Section. In a typical synthesis, 1 mmol of $CuCl_2 \cdot 2H_2O$ and 1 mmol of $Na_2S_2O_3 \cdot 5H_2O$ was dissolved into ammonia solution to form a dark blue solution (final concentration: $[Cu^{2+}] = [S_2O_3^{2-}] = 0.025$ M, $[NH_3] = 6.7$ M). The solution was then transferred into a 60 mL Teflon-lined stainless steel autoclave, kept at 150 °C for 12 h, and cooled down to room temperature naturally. The dark products were filtered off, washed with deionized water and absolute ethanol several times, and then dried in a vacuum at 60 °C for 4 h.

The X-ray powder diffraction patterns (XRD) of the products were measured using a Shimadzu X-ray diffractometer (XRD-6000). The morphology and structure of the sample were characterized by scanning electron microscopy (SEM, Hitachi S-4800 at 5 kV) and transmission electron microscopy (TEM, JEOL 2010 at 200 kV). An X-ray energy dispersive spectrum (EDS) was taken with a Hitachi S-4800 SEM with an acceleration voltage of 15 kV.

Results and Discussion. In Figure 1, the XRD pattern of the product can be indexed to a pure hexagonal (high chalcocite) Cu_2S phase with a lattice parameter a = 3.924 Å, c = 6.717 Å (space group: $P6_{3/mmc}$), which is consistent with the JCPDS card No. 84-0209. Although the high chalcocite phase is only stable at high temperature, and will transform into a low chalcocite with monoclinic phase at 103 °C,[33] the hexagonal phase is thermodynamically favored at our synthetic temperature and can be kept metastable at room temperature. EDS analysis shows that the mean atom ratio of Cu/S in the final product is 2:1 (see the Supporting Information, Figure S1). The XRD pattern and EDS spectrum indicates a pure hexagonal phase Cu_2S was obtained under our experimental conditions without impurities.

Figure 2a is the low magnification SEM images of products, which illustrates that the products are composed of a hexagram structure with a diameter of about 6−10 μm. A high magnification SEM image in Figure 2b indicates that the adjacent angles of the shuttle-like branches are 60° with a 6-fold rotation axis at their center. Moreover, mirror symmetry is found to be perpendicular to the hexad axis. The SEM image of the side surface of DFHD in

*To whom correspondence should be addressed. E-mail: fzfscn@mail.ahnu.edu.cn (Z.F.); jmshen@ustc.edu (J.S.). Tel: +86 553 3937135. Fax: +86 553 3869302.

Published on Web 12/31/2009

Figure 2c also demonstrates the mirror symmetry between two layers as mentioned above. In addition to the 6-fold principal axis and horizontal mirror plane perpendicular to it, six 2-fold axes are also found to be perpendicular to the 6-fold principal axis. Judging from the above-mentioned factors, it can be concluded that the symmetry of the Cu_2S DFHD structure is D_{6h} (Figure 2d).[34] The TEM image also illuminates its hexagonal structure with a 6-fold rotation axis (Figure 2e). The branch is about 1.3 μm in length and 370 nm in width. The diameter deviation of DFHD measured from three different directions is about 5.7%, which indicates high structural consistency of the products. Selected area electron diffraction (SAED) in Figure 2f, recorded along the [0001] zone axis on one branch, indicates that the branch of hexagonal DFHD grows along the [11$\bar{2}$0] direction.

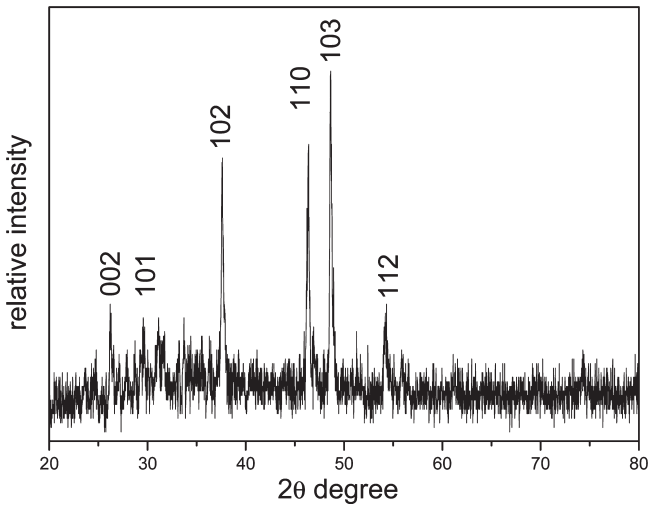

Figure 1. XRD pattern of the obtained product.

In the process of our reaction, the influence of reaction parameters, such as the type and concentration of reagents, reaction temperature, and time, have been found to have a great influence on the structure and morphology of the final product. Thus, we have carried out a series of supplementary experiments to investigate the mechanism that dominates the formation of the unusual DFHD microstructures. Ligands have been used to control the morphology of nanomaterials for their coordination ability with metal cations or selective adsorption on some crystal surfaces.[35] In our synthesis strategy, ammonia, as a medium strong ligand, also has an important effect on the morphology of the final products. Without the addition of ammonia solution, only irregular flakes were obtained, as shown in Figure 3a. Ammonia solutions of different concentrations were used to evaluate their effects on the morphology of the products with other reaction parameters unchanged. When the concentration of ammonia was 1.67 M, the final products were six-rowed microprisms (Figure 3b). Gear-like microstructures with a height of about 800 nm and a diameter of about 2 μm were synthesized with increasing ammonia concentration to 3.35 M. (Figure 3c). Compared with the DFHD products in 6.7 M ammonia, the growth rate of the (11$\bar{2}$0) plane was obviously slowed down under lower ammonia concentration. We further used concentrated ammonia solution as solvent and obtained snowflake-like microstructures (Figure 3d) with a diameter of ~20 μm. It is obvious that the concentration of ammonia has a strong influence on the growth rate of the (11$\bar{2}$0) crystalline plane and thus affects the final morphology of Cu_2S microcrystals. A plausible explanation to this phenomenon could be that the existence of ammonia in the reaction system might stabilize the (0001) crystalline plane of Cu_2S and make the crystal growth along the high-index {11$\bar{2}$0} crystalline planes. These observations clearly show that the presence of ammonia is beneficial to the control of the morphology

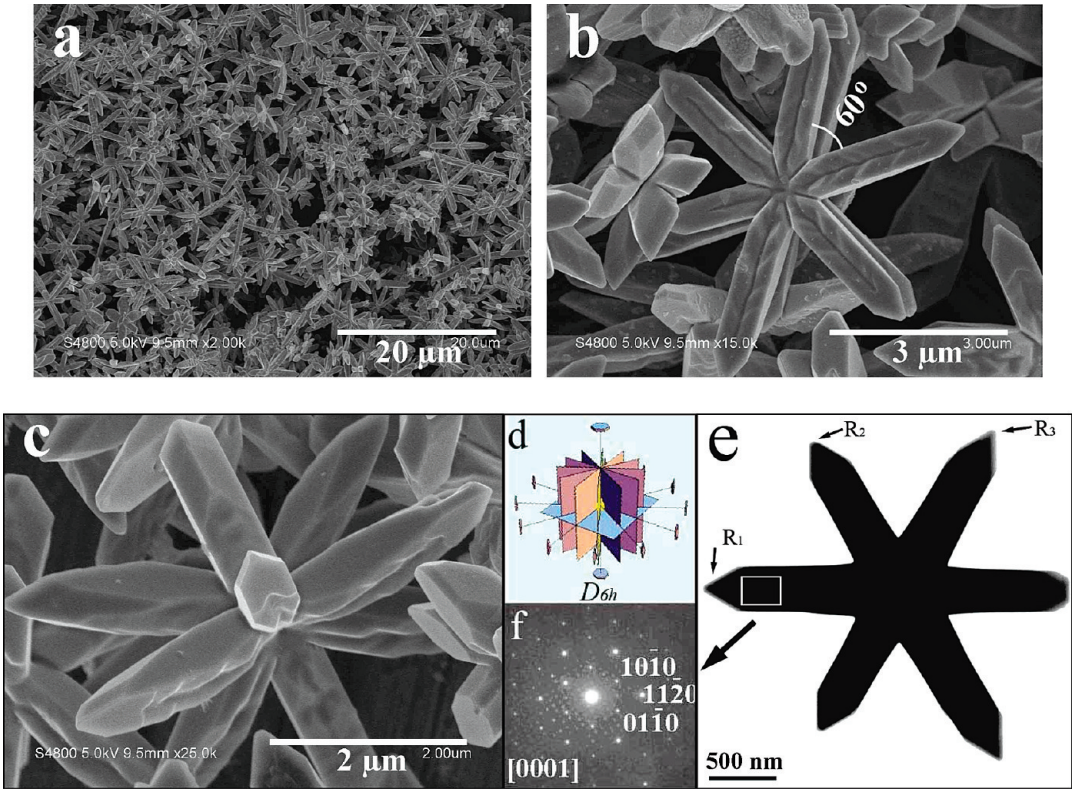

Figure 2. (a) The general morphology of the Cu_2S products. (b) The high magnification of obverse side of DFHD. (c) The side view of DFHD. (d) The point group D_{6h}. (e) TEM image of a single DFHD. (f) SAED of the DFHD.

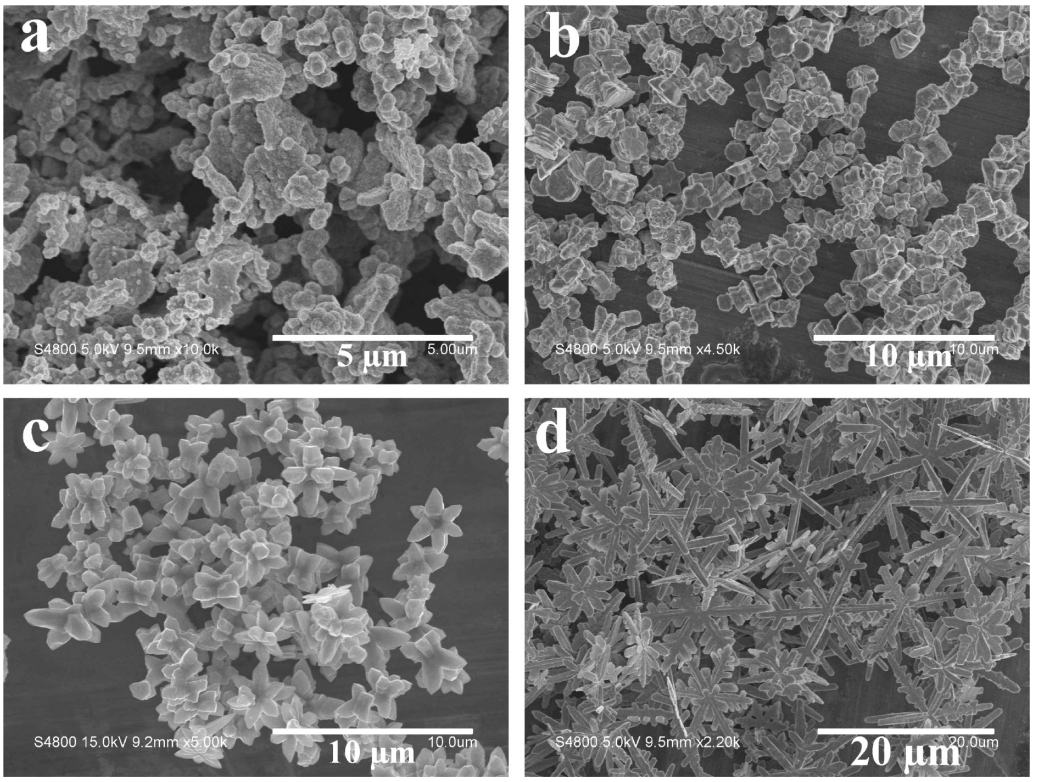

Figure 3. SEM image of the products obtained under different ammonia concentrations. (a) 0 M, (b) 1.67 M, (c) 3.35 M, (d) 13.4 M.

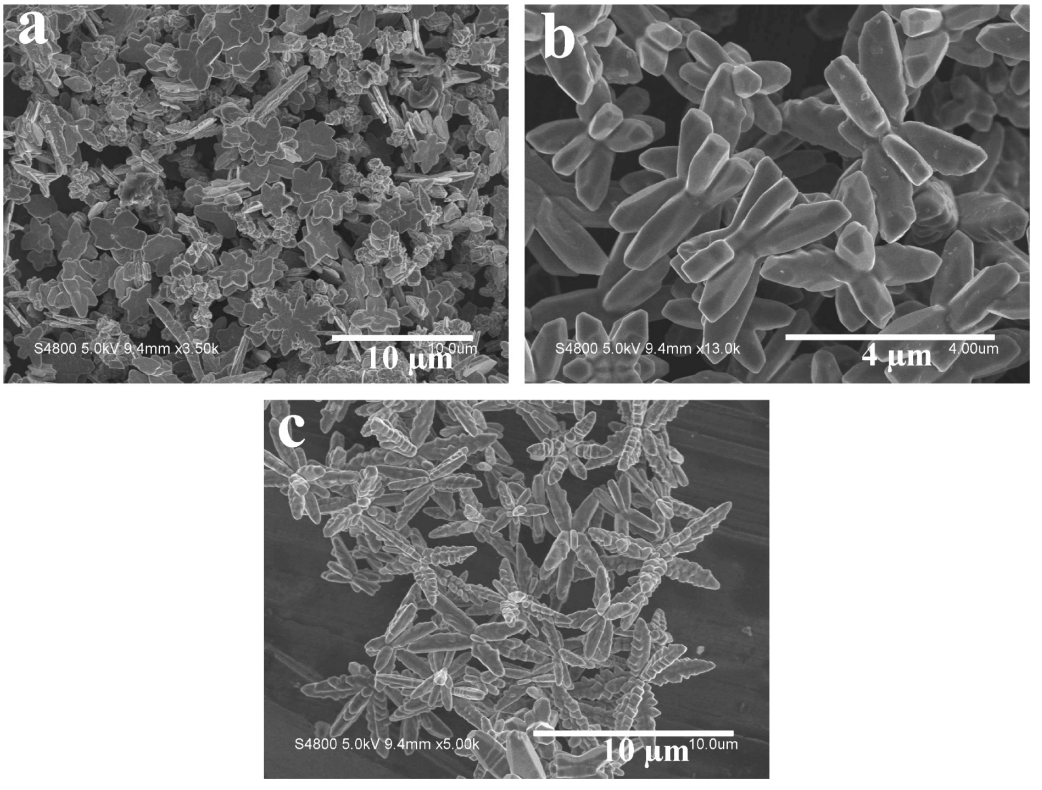

Figure 4. SEM images of the products obtained at different Cu^{2+} concentrations. (a) 0.0125 M, (b) 0.05 M, (c) 0.1 M.

of the final products. Nevertheless, when ammonia was replaced by ethylenediamine, a ligand with stronger polarity and chelation ability, in the reaction, only nanoplatelets were formed in ethylenediamine solutions at various concentrations (Figure S2 in Supporting Information). We believe that the reason may be attributed to the strong chelation ability of ethylenediamine that has strong effects on the nucleation and growth rate of Cu_2S crystals.

We have also adjusted the concentration of Cu^{2+} to examine its effect on the final product. Figure 4a is the SEM image of the hexagram-like microcrystals obtained at a Cu^{2+} concentration of 0.0125 M. When the Cu^{2+} concentration increased to 0.05 M, the

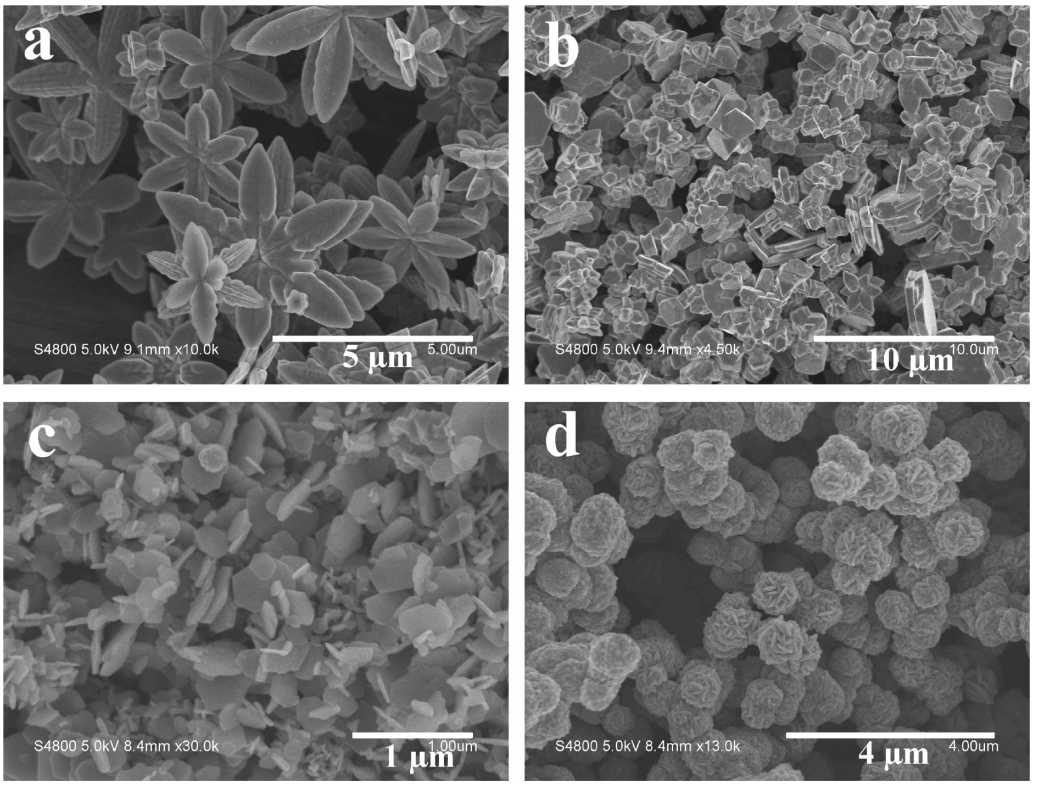

Figure 5. SEM images of the products obtained under (a) 120 °C, (b) 180 °C. Using a different sulfur source under 150 °C for 12 h: (c) thioacetamide, (d) thiourea.

product is completely composed of multiped microstructures (Figure 4b). Further increasing the Cu^{2+} concentration to 0.1 M, the branches of the multiped structures become longer and the hierarchical structure appear as shown in Figure 4c. We believe that the reason for this phenomenon is due to the growth rate of the [0001] plane is proportional to the Cu^{2+} concentration. Thus, the multiped structures with the [112$\bar{z}$] growth direction are formed instead of DFHDs. It can be concluded that the concentrations of ammonia and copper ions determine the z value in the growth direction [112$\bar{z}$]. In addition, the anions of the copper sources do not affect the final morphology greatly; for example, DFHDs could be obtained no matter whether $Cu(NO_3)_2 \cdot 3H_2O$ or $CuSO_4 \cdot 5H_2O$ was used (see the Supporting Information, Figure S3).

In addition to the reagents, temperature also plays a crucial role in the reaction process. No product could be obtained when the synthesis was carried out below 100 °C, for $Na_2S_2O_3$ only decomposes at a temperature higher than 100 °C. Thus, we further examined the products obtained at 120 and 180 °C, respectively. As shown in Figure 5a, although the DFHDs could be also produced at 120 °C, the branches become as thin as a leaf. When the reaction temperature was elevated to 180 °C, only irregular particles were synthesized (Figure 5b). We speculate that the intensity of the coordinate bond between Cu^{2+} and NH_3 might be greatly weakened at elevated temperature, while the decomposition rate of $S_2O_3^{2-}$ is accelerated, which results in a relatively faster growth rate and the formation of irregular particles. It is noticed that $[S_2O_3]^{2-}$ has similar chelation ability with ammonia when it interacts with Cu^{2+}.[36,37] As a result, the sulfur source may affect the final morphology of products. In fact, the hexagonal flakes (Figure 5c) and nanospheres (Figure 5d) can be obtained when $Na_2S_2O_3$ was replaced by thioacetamide and thiourea, respectively. In our synthesis strategy, we believe that the role of $S_2O_3^{2-}$ in the synthesis of Cu_2S DFHDs is as follows: (i) reduce the $[Cu(NH_3)_4]^{2+}$ to $[Cu(NH_3)_2]^{+}$,[38] and (ii) serve as a sulfur source. From the above results, the morphology and structure of the final product are determined by the presence of $[S_2O_3]^{2-}$, the concentration of reagents, and ammonia. The co-coordination effect of the two ligands makes the final morphology of Cu_2S distinguished. However, the product's morphology was not sensitive to the concentration of $Na_2S_2O_3$ or other thiosulfate (Figure S4 in Supporting Information). It may be because the release rate of S^{2-} via decomposition of $S_2O_3^{2-}$ remains almost invariable at the same experimental temperature.

Previous studies have proven that the morphologies of crystals depend on the deviation degree of formation conditions from equilibrium.[39] Under equilibrium conditions, the crystal usually has one unique morphology with a low index plane to achieve the lowest surface free energy. As the system is driven further from equilibrium, mass transport of material plays a key role in determining crystal shapes. Dendritic growth will be promoted under this environment when the mass transport rate of ions or molecules that feeds the growing crystals is lower than the growth rate of crystals.[40−42] The regularity of dendrites that depend on a crystallographic symmetry appears when the driving force of crystallization including supersaturation and supercooling is relatively low.[43] In our experimental conditions, the mass transport rate of Cu^{2+} is confined by ammonia because of its medium strong coordination effect. In order to investigate the formation process of the DFHDs, we have performed a typical synthesis process at 150 °C for 2 and 6 h, respectively. Temporal morphological evolution is followed by SEM observation, as shown in Figure 6. The DFHD is formed even in 2 h and further grows into larger and more refined structures along with a prolonged reaction time. However, the quantity of the product is less than that obtained at 150 °C for 12 h. The result indicates that the mass transport rate of Cu^{2+} that feeds the growing Cu_2S dendrites has been greatly slowed down for the coordination effect under this nonequilibrium condition. For the same reason, the morphology of dendrites will change accordingly with the concentration of reagent that may affect the mass transport rate including ammonia and Cu^{2+}. Figure 7 depicts the final structure which is summarized

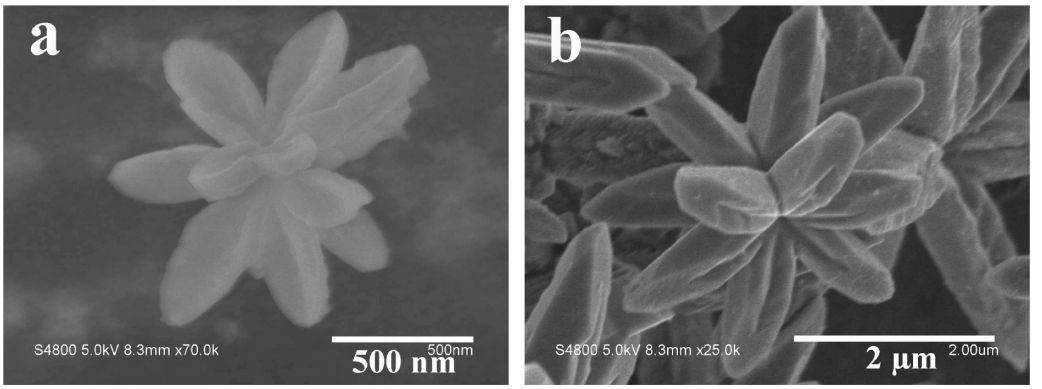

Figure 6. Formation processes of Cu_2S DFHDs. SEM images after hydrothermal treating for (a) 2 h, (b) 6 h.

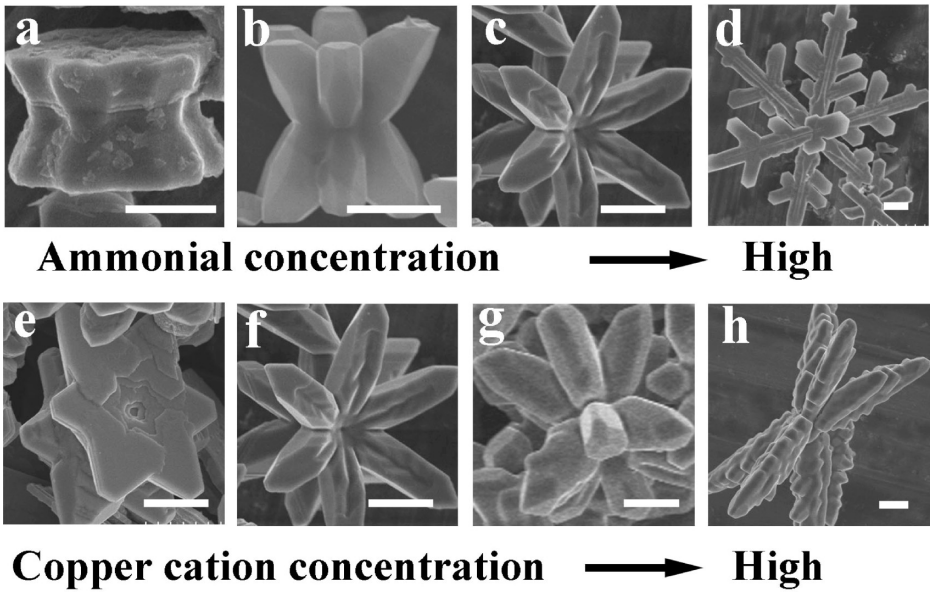

Figure 7. A summary of various dendrites of Cu_2S under the current synthetic conditions (a−h: scale bar = 1 μm). (a) Six-rowed prism. (b) Gear like structure. (c, f) Double fold hexagonal dendrite. (d) Snowflake. (e) Double fold hexagram. (g) Multiped structure with 12 legs. (h) Multiped structure with longer legs.

as a function of starting ammonia and copper action concentrations. On the basis of our experiments, the branching growth habit is sensitive to the chemical environment provided, which determines the morphology of the final Cu_2S DFHD microcrystals.

Conclusions. In conclusion, Cu_2S DFHD microstructures with D_{6h} symmetry have been successfully synthesized through a simple ammonia-assisted hydrothermal route. The influences of reaction parameters, such as the ligand type, the concentration of reagents, and the precursor of sulfur, on the morphology and structure of the final products have been thoroughly discussed. A possible nonequilibrium mechanism has been proposed to elucidate the formation of this unconventional microstructure on the basis of our experimental results. This work provides not only a simple bottom-up approach to synthesize inorganic materials with a complex structure but also a benefit to the study of dendritic growth.

Acknowledgment. The authors thank Dr. Zhenghua Wang for fruitful discussions. We are also grateful for the financial support from the National Natural Science Foundation of China (20701002), Science and Technological Fund of Anhui Province for Outstanding Youth (08040106834), and the Education Department of Anhui Province (No. 2006KJ006TD).

Supporting Information Available: EDS spectra, SEM images of the products at different synthesis conditions. This material is available free of charge via the Internet at http://pubs.acs.org.

References

(1) Gravner, J.; Griffeath, D. *Exp. Math.* **2000**, *15*, 421.
(2) Witten, T. A.; Sander, L. M. *Phys. Rev. Lett.* **1981**, *47*, 1400.
(3) Langer, J. S. *Rev. Mod. Phys.* **1980**, *52*, 1.
(4) Wang, S. Z.; Xin, H. W. *J. Phys. Chem. B* **2000**, *104*, 5681.
(5) Schulze, T. P. *Phys. Rev. E* **2008**, *78*, 020601.
(6) Chernov, A. A. *J. Cryst. Growth* **1974**, *24/25*, 11.
(7) Kuroda, T.; Irisawa, T.; Ookawa, A. *J. Cryst. Growth* **1977**, *42*, 41.
(8) López, C. M.; Choi, K. S. *Langmuir* **2006**, *22*, 10625.
(9) Fang, J. X.; Hahn, H.; Krupke, R.; Schramm, F.; Scherer, T.; Ding, B. J.; Song, X. P. *Chem. Commun.* **2009**, 1130.
(10) Zhou, X. M.; Wei, X. W. *Cryst. Growth Des.* **2009**, *9*, 7.
(11) Zhu, Y. C.; Zheng, H. G.; Yang, Q.; Pan, A. L.; Yang, Z. P.; Qian, Y. T. *J. Cryst. Growth* **2004**, *260*, 427.
(12) Bernard, C. H.; Tan, H.; Fang, W. Y. *Langmuir* **2006**, *22*, 9712.
(13) Corno, J. A.; Stout, J.; Yang, R. S.; Gole, J. L. *J. Phys. Chem. C* **2008**, *112*, 5439.
(14) Yu, S. H.; Chen, S. F. *Curr. Nanosci.* **2006**, *2*, 81.

(15) Xu, F.; Zhang, P.; Navrotsky, A.; Yuan, Z. Y.; Ren, T. Z.; Halasa, M.; Su, B. L. *Chem. Mater.* **2007**, *19*, 5680.
(16) Chen, D.; Ye, J. H. *Adv. Funct. Mater.* **2008**, *18*, 1922.
(17) Du, W. M.; Qian, X. F.; Ma, X. D.; Gong, Q.; Cao, H. L.; Yin, J. *Chem.—Eur. J.* **2007**, *13*, 3241.
(18) Ueda, K.; Takafuji, K.; Hiramatsu, H.; Ohta, H.; Kamiya, T.; Hirano, M.; Hosono, H. *Chem. Mater.* **2003**, *15*, 3692.
(19) Yao, Z. Y.; Zhu, X.; Wu, C. Z.; Zhang, X. J.; Xie, Y. *Cryst. Growth Des.* **2007**, *7*, 1256.
(20) Sigman, M. B.; Ghezelbash, A.; Hanrath, T.; Saunders, A. E.; Lee, F.; Korgel, B. A. *J. Am. Chem. Soc.* **2003**, *125*, 16050.
(21) Gao, J. N.; Li, Q. S.; Zhao, H. B.; Li, L. S.; Liu, C. L.; Gong, Q. H.; Qi, L. M. *Chem. Mater.* **2008**, *20*, 6263.
(22) Zhuang, Z. B.; Peng, Q.; Zhang, B. C.; Li, Y. D. *J. Am. Chem. Soc.* **2008**, *130*, 10482.
(23) Wang, K. J.; Li, G. D.; Li, J. X.; Wang, Q.; Chen, J. S. *Cryst. Growth Des.* **2007**, *7*, 2265.
(24) Lim, W. P.; Low, H. Y.; Chin, W. S. *Cryst. Growth Des.* **2007**, *7*, 2429.
(25) Yu, X. L.; Cao, C. B.; Zhu, H. S.; Li, Q. S.; Liu, C. L.; Gong, Q. H. *Adv. Funct. Mater.* **2007**, *17*, 1397.
(26) Liu, Z. P.; Liang, J. B.; Xu, D.; Lu, J.; Qian, Y. T. *Chem. Commun.* **2004**, 2724.
(27) Jiao, S. H.; Xu, L. F.; Jiang, K.; Xu, D. S. *Adv. Mater.* **2006**, *18*, 1174.
(28) Lubeck, C. R.; T. Han, Y. J.; Gash, A. E.; Satcher, J. H.; Doyle, F. M. *Adv. Mater.* **2006**, *18*, 781.
(29) Wang, X. Y.; Fang, Z.; Lin, X. *J. Nanopart. Res.* **2009**, *11*, 731.
(30) Wu, Z. C.; Pan, C.; Yao, Z. Y.; Zhao, Q. R.; Xie, Y. *Cryst. Growth Des.* **2006**, *6*, 1717.
(31) Knoxville, T. N., John A. D. *Lange's Chemistry Handbook Version 15*; McGraw-Hill: New York, 1999.
(32) Wu, C. Y.; Yu, S. H.; Antonietti, M. *Chem. Mater.* **2006**, *18*, 3599.
(33) Larsen, T. H.; Sigman, M.; Ghezelbash, A.; Doty, R. C.; Korgel, B. A. *J. Am. Chem. Soc.* **2003**, *125*, 5638.
(34) Qian, Y. T. *Introduction to Crystallography*; University of Science and Technology of China Press: Hefei, China, 1999 (in Chinese).
(35) Deng, Z. X.; Wang, C.; Sun, X. M.; Li, Y. D. *Inorg. Chem.* **2002**, *41*, 869.
(36) Fischmann, A. J.; Warden, A. C.; Black, J.; Spiccia, L. *Inorg. Chem.* **2004**, *43*, 6568.
(37) Simonescu, C. M.; Carp, O.; Patron, L.; Capatina, C. *J. Optoelectron. Adv. Mater.* **2008**, *10*, 2700.
(38) Briones, R.; Lapidus, G. T. *Hydrometallurgy* **1998**, *50*, 243.
(39) Mann, S. *Angew Chem. Int. Ed.* **2000**, *39*, 3392.
(40) Devon, R.; Figura, J. R.; Douthat, D.; Kudenov, J.; Maselko, J. *Chem. Commun.* **2005**, 1678.
(41) Matsushita, M.; Sano, M.; Hayakawa, Y.; Honjo, H.; Sawasa, Y. *Phys. Rev. Lett.* **1984**, *53*, 286.
(42) Chen, X. Y.; Wang, X.; Wang, Z. H.; Yang, X. G.; Qian, Y. T. *Cryst. Growth Des.* **2005**, *5*, 347.
(43) Oaki, Y.; Imai, H. *Cryst. Growth Des* **2003**, *3*, 711.